TECHNICAL ARTICLE

SIMULATION 74:6, 351-358

ISSN 0037-5497/00
Printed in the United States of America

Flow Simulation in Stochastic Porous Media

C.T.J. Dodson
Department of Mathematics
University of Manchester Institute of Science and Technology (UMIST)
P.O. Box 88, Manchester, M60 1QD, United Kingdom
email: dodson@umist.ac.uk

W.W. Sampson
Department of Paper Science
University of Manchester Institute of Science and Technology (UMIST)
P.O. Box 88, Manchester, M60 1QD, United Kingdom
email: w.sampson@umist.ac.uk

A family of gamma distributions can be used to model the pore size distributions in a range of stochastic porous media. Our simulator generates distributional and net flow data for different fluid flow regimes through such networks. The outputs from the simulation show strong relationships between mean flow and the variance of pore radii for turbulent, laminar, molecular and capillary flow. We observe also affine relationships between the coefficient of variation of local flow rate and the variance of pore radii for each of the above flow modes.

Keywords: Please provide up to eight

1. Introduction

The flow of fluids through any system is controlled by its geometry, the driving force and the properties of the fluid. In a stochastic porous material the observable geometry of the system will vary from region to region, and this manifests itself in a distribution of local porosities and of local pore size distributions. Statistical geometry has been employed by several authors to describe the pore size distribution in random fibre networks, an important class of stochastic porous media used as fluid barriers and filters. The work of Miles [1] was extended by Corte and Lloyd [2], who used the negative exponential distribution to model the distances between fibre crossings in a random network of fibres with uniform orientation. They obtained the analytic result that for such networks, the distribution of pore radii is lognormal; also, for different values of the mean distance between fibre crossings, the standard deviation of pore radii is proportional to the mean.

Real fibre networks such as paper and non-woven filter media have nonrandom structures, primarily as a consequence of interactions between fibres in the suspensions from which the network is formed. These interactions cause fibre clumping which results in a greater variance of local areal density than found in a

random network formed from the same fibres [3]. The structure of fibre networks in suspension and the influence of clumping on their geometry is discussed in [4]. The clumping effect has consequences for the pore size distribution in the network, and decreased mass uniformity is associated with an increase in mean and variance of pore radii. The pore size distribution in non-random fibre networks has been modelled by Dodson and Sampson [5, 6] who used a gamma distribution to describe the distances between fibre crossings. Precise expressions for the probability density functions for pore areas and pore radii are given in [5, 6]; however, these functions are themselves well approximated by gamma distributions [6]. Whilst these results have been derived for fibre networks, there is some evidence that the gamma distribution may be used to describe also the pore radius distribution in granular packings and other stochastic porous media [7, 8].

The volumetric flow rate, q through a given cylindrical pore of radius, r is proportional to r^m where the exponent $m = 4, 3, 2, \frac{1}{2}$, depending on whether the flow is laminar, molecular (Knudsen), turbulent or capillary, respectively. The coefficients of r^m are dependent on fluid properties, such as viscosity and surface tension, additional geometric parameters such as capillary length and the driving force; full expressions are given in [9] along with a discussion of the appropriate use of each. Measurements of pore radius distribution using fluid permeation, such as those described by Corte [10] and in ASTM methods [11], are based on models of porous media as bundles of parallel straight capillaries. The relationship between the size of pores measured by such techniques and their geometrical size is complex, as the void space within a porous material is typically tortuous and interconnected; tortuosity has been shown by Foscolo et al. [12] to be inversely proportional to porosity. What is clear, however, is that the agreement between geometric theory, derived for two-dimensional structures, and flow-based measurements on real materials, which may have a significant structural component in the third dimension, is good [6, 7, 8, 13].

We expect therefore that the structural nonuniformity of a planar stochastic porous medium will give rise to nonuniformity of flow perpendicular to its plane. Such effects have been inferred from measurements of structural uniformity in fibre networks formed in the laboratory [14] and on a pilot scale paper machine [15]. However, direct measurement of flows through fibre networks at small scales, and hence their distribution, is difficult to realise. Here we present a simulation of local flow rates through zones in a planar porous medium with gamma-distributed pore radii. The results of the simulation have relevance to the uptake of viscous inks and wetting agents in printing processes and to industrial and laboratory filtration processes.

2. Simulation

The objective of our simulation is to generate data for the flow of fluids under different regimes through planar zones containing circular voids. We consider the incidence of voids within a zone to be a Poisson process such that:

$$f(n_p) = \frac{e^{-\overline{n}_p}\,\overline{n}_p^{\,n_p}}{n_p!} \tag{1}$$

where n_p is the number of pores in a zone and $\overline{n}_p$ is the mean number of pores in a zone; as n_p is a Poisson-distributed variable, $\overline{n}_p$ is also the variance of the number of pores in a zone.

Based on the experience of experimental data and modelling [6, 8], we consider the broadly applicable case of gamma-distributed pore radii. As our interest is the effect of the variance of pore radii on the variance of flow through zones, we use the normalised gamma distribution given by equation:

$$g(r) = \frac{k^k}{\Gamma(k)}\, r^{k-1}\, e^{-kr} \tag{2}$$

which has mean, $\overline{r} = 1$, and variance, $\sigma^2(r) = \frac{1}{k}$. The normalised gamma distribution has been applied also in recent papermaking simulations [16]. A consequence of increasing the variance of pore radii at constant n_p is to increase also the total area of pores, $\sum_i \pi r_i^2$ in a zone and hence its porosity; naturally, an increased porosity will have a reduced resistance to flow. The first stage of the simulation therefore was to establish a relationship between k and the mean open area for all zones; given such a relationship, calculations could be performed weighting $\overline{n}_p$ by some suitable function of k to allow constant mean open area for all k. Simulations have been carried out using Mathematica [17] which has been chosen for its list handling and graphics generation capabilities. The routine generates a list of length, n_{zones}, where each element of the list is a sublist of normalised gamma distributed random numbers with variance, $\frac{1}{k}$; the lengths of the sublists are Poisson-distributed with mean, $\overline{n}_p$. The sum of the squares of the elements of the sublist is the area of pores in each zone divided by π.

Figure 1 shows $\overline{A}_{norm}$, the mean open area normalised by that at $k = 1$, for $n_p = 5$, 10, 20, 40 and 60 and for $n_{zones} = 5000$, plotted against the variance of pore radii, $\frac{1}{k}$.

The regression:

$$\overline{A}_{norm} = 0.4984 + 0.4896\frac{1}{k} \tag{3}$$

fits the data in Figure 1 with coefficient of determination, $R^2 = 0.9997$. Thus, to ensure constant open area in subsequent simulations, the number of pores in a zone is given as a function of k:

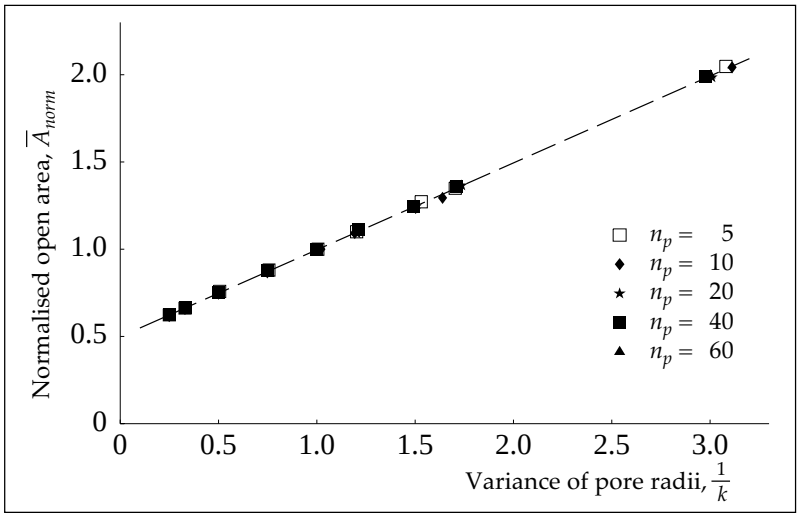

Figure 1. Relationship between normalised mean zone open area, $\overline{A}_{norm}$ and variance of pore radii, $\frac{1}{k}$. *Normalisation is to* $\overline{A}_{norm} = 1$ *at* $n_p = 1$; *the relationship is used to generate zones with constant porosity for all pore size distributions.*

$$n_p(k) = 2\, n_p(1)\, \frac{k}{1+k} \qquad (4)$$

where $n_p(1)$ is the value of n_p at $k = 1$.

Using Equation (4), a new set of lists was generated as described above, though the length of the sublists were now Poisson-distributed with mean, $\overline{n}_p(k)$. The data of Corte and Lloyd [2] for paper sheets shows the coefficient of variation of pore radii to be in the range of 40% to 100%. In the early stages of paper forming we have the expectation that this variance will be greater; accordingly we have used the range $\frac{1}{3} \le \frac{1}{k} \le 3$ for all the simulations presented here and this should cover the range of pore size distributions found in commercial fibre networks during and after their manufacture.

The mean flow rate through each zone was calculated as the sum of the elements of a sublist, each raised to the appropriate power for a given flow rate. In summary, the procedure for each simulation was as follows:

1. Generate a list of length n_{zones}, each element of the list being an integer, $n_{p,i}$ selected at random from a Poisson distribution with mean $n_p(k)$. Each element in the list represents the number of pores in a zone.
2. Generate a list of length n_{zones} of sublists of length $n_{p,i}$, each element of the sublists being selected at random from a gamma distribution with unit mean and variance $\frac{1}{k}$. Thus, the length of each sublist is the number of pores in a zone, and the elements in each sublist represent pore radii; the number of sublists is the number of zones.
3. Raise each element of the sublists to the power m, where m is determined by the flow regime of interest. The elements of each sublist are a number proportional to the flow in each pore.
4. Sum the elements of each sublist. The output is a list of length n_{zones} where each element has a value proportional to the flow rate through a zone.
5. Normalise the list by the mean value at $k = 1$ to yield a list of length n_{zones} where each element represents the flow through a zone as a multiple of the mean flow rate at $k = 1$.
6. Process data to determine mean, variance and coefficient of variation of local flow rate. Count number of zones having flows in given class ranges to yield distributional flow plots as shown, for example, in Figure 2.

To investigate the effect of different flow regimes on a given structure, stages 3 through 6 where carried out for different values of m using the lists generated in stages 1 and 2.

An example of the output from the simulator is shown in Figure 2 which gives, for the turbulent regime, the frequency of normalised local flow rates, $P(\overline{q}_{norm})$ where the normalisation is by the mean local flow rate at $k = 1$. Subsequent figures and discussion are based on the characterising statistics for such distributions of local flow rates.

Figure 3 shows the normalised mean flow rate, $\overline{q}_{norm}$ for turbulent flow plotted against the variance of pore radii, $\frac{1}{k}$ for $n_p(1) = 10$, 20, 40 and 60; normalisation of mean flow rate is to that for $n_p(1) = 20$. The value of n_{zones} for this, and all simulations presented here, was 5000.

We note that Figure 3 represents also the normalised mean open area $\overline{A}_{norm}$ because the flow rate in turbulent mode is proportional to pore radius to the power

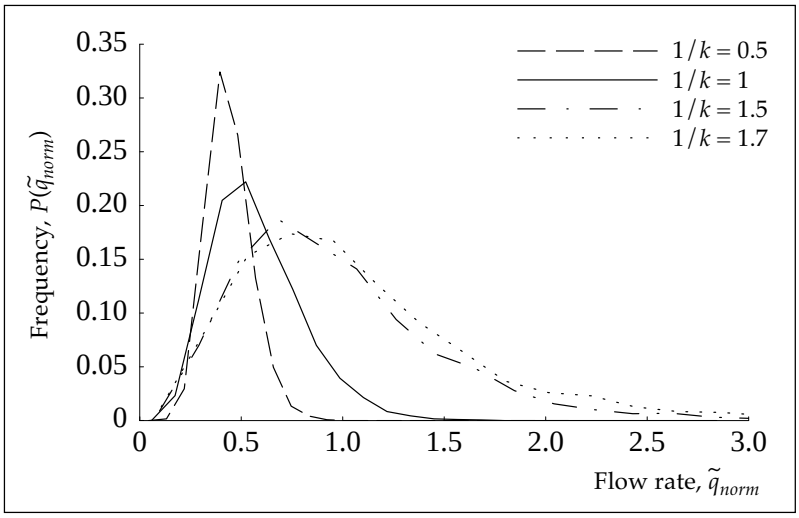

Figure 2. The effect of variance of pore radii on the distribution of local flow velocities for turbulent flow. *Flow rates normalised to the mean at* $k = 1$.

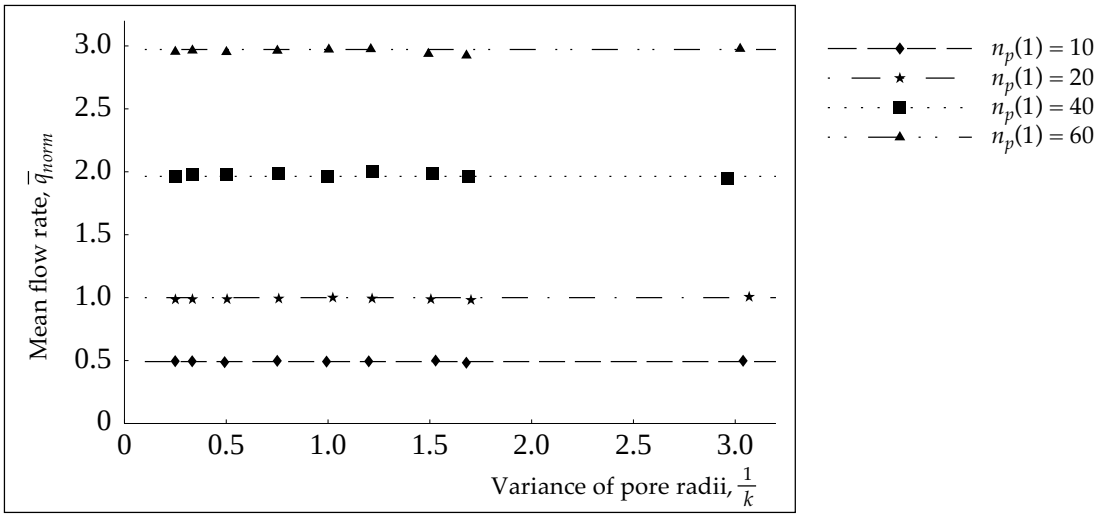

Figure 3. Relationship between normalised mean flow rate, $\bar{q}_{norm}$ and variance of pore radii, $\frac{1}{k}$ for turbulent flow. *The mean turbulent flow rate is independent of the variance of pore radii.*

$m = 2$. The coefficient of variation of local flow rate, $CV(\tilde{q})$ for turbulent flow is plotted against $\frac{1}{k}$ in Figure 4 for $n_p(1) = 10$, 20, 40 and 60; the same values of $n_p(1)$ are used for all the simulations presented. The plots illustrate an affine relationship between $CV(\tilde{q})$ and $\frac{1}{k}$ with the gradient decreasing as the mean number of pores in a zone increases; the coefficient of determination for the fit is greater that 0.996 in all cases. Also, at a given value of $\frac{1}{k}$, $CV(\tilde{q})$ decreases as the mean number of pores increases; this might be expected as increasing the value of parameter, $n_p(1)$ is consistent with increasing the size of the inspection zone within a given structure or increasing the mean number of pores within inspection zones of constant size.

Figures 5 and 6 show the normalised mean flow rate and coefficient of variation of local flow rate for laminar flow, i.e., $m = 4$. For the normalised mean laminar flow rate the fitted curves are second-order polynomials and fit with coefficients of determination greater than 0.998. The affine relationship between the coefficient of variation and $\frac{1}{k}$ is less strong than that observed for turbulent flow with coefficients of determination between 0.743 at $n_p(1) = 20$ and 0.991 at $n_p(1) = 60$. The coefficients of variation for laminar flow are noticeably higher than those for turbulent flow; this, and the weaker correlation with $\frac{1}{k}$, being due to the high value of the exponent m and hence the substantial contribution of large pores to flow.

Figures 7 and 8 show the normalised mean flow rate and coefficient of variation of local flow rate for capillary flow, i.e., $m = \frac{1}{2}$. For the normalised mean capillary flow rate the fitted curves are of the form $a + b e^{-\frac{1}{k}}$ and fit with coefficients of determination greater than 0.998.

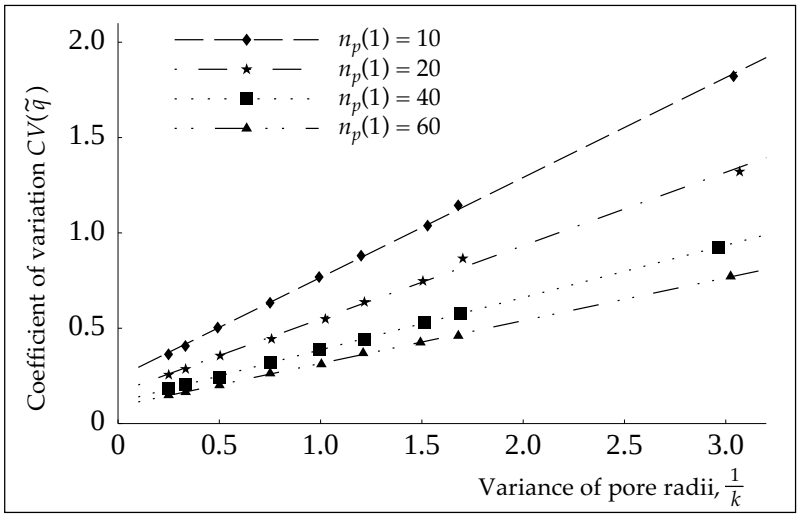

Figure 4. Relationship between coefficient of variation of local flow rate, $CV(\tilde{q})$ and variance of pore radii, $\frac{1}{k}$ for turbulent flow. *The variance of local flow rate for turbulent flow exhibits an affine relationship with the variance of pore radii.*

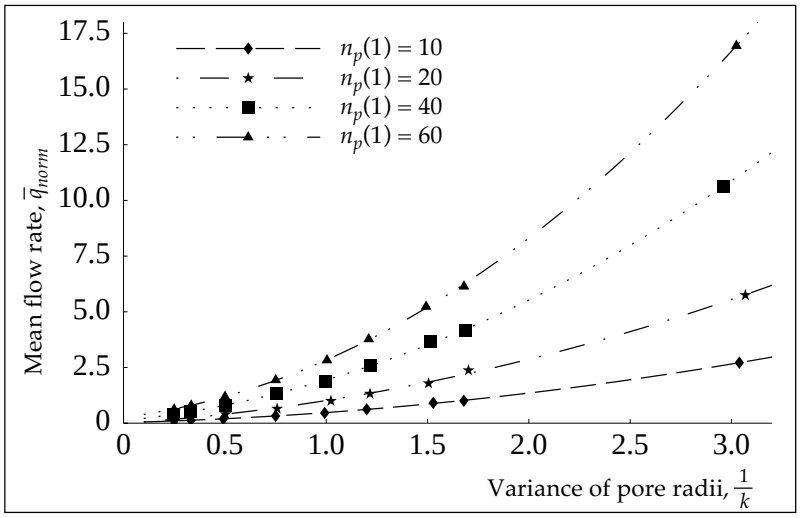

Figure 5. Relationship between normalised mean flow rate, $\overline{q}_{norm}$ and variance of pore radii, $\frac{1}{k}$ for laminar flow. *At constant porosity, the increase in mean flow rate with increasing variance of pore radii is characterised well by second order polynomials.*

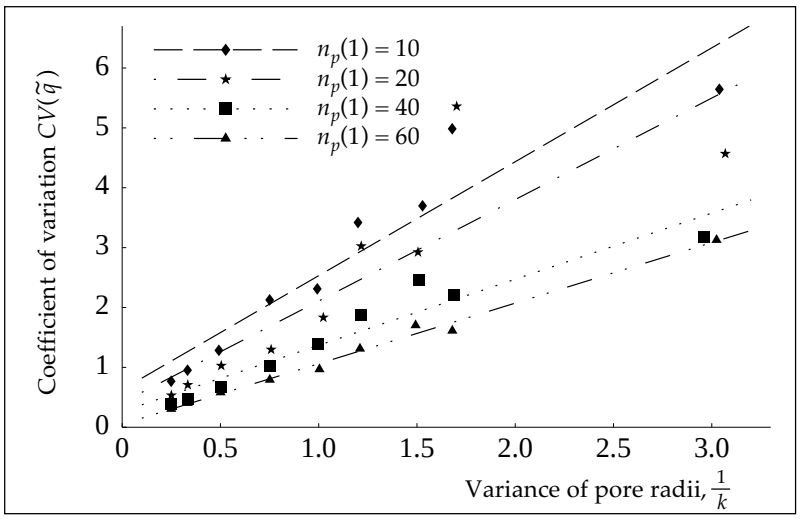

Figure 6. Relationship between coefficient of variation of local flow rate, $CV(\tilde{q})$ and variance of pore radii, $\frac{1}{k}$ for laminar flow. *The affine relationship is weaker than for turbulent flow particularly for larger, or more porous, zones.*

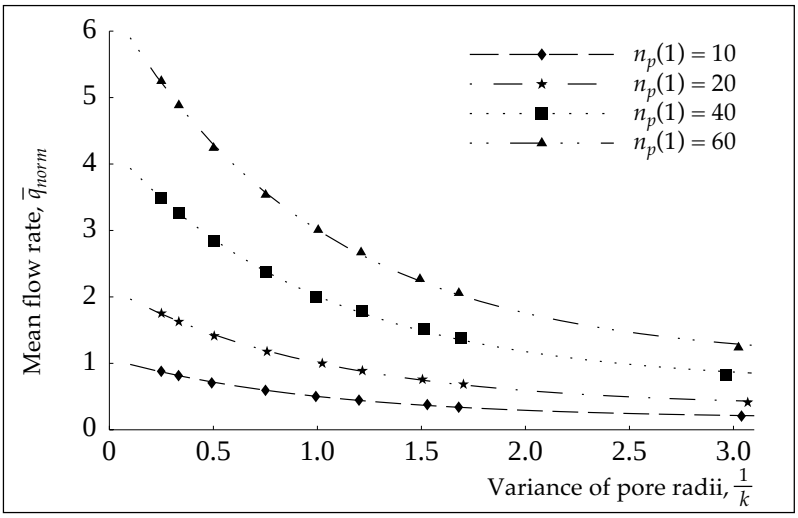

Figure 7. Relationship between normalised mean flow rate, $\overline{q}_{norm}$ and variance of pore radii, $\frac{1}{k}$ for capillary flow. *Mean flow rate decreases exponentially with increasing variance of pore radii.*

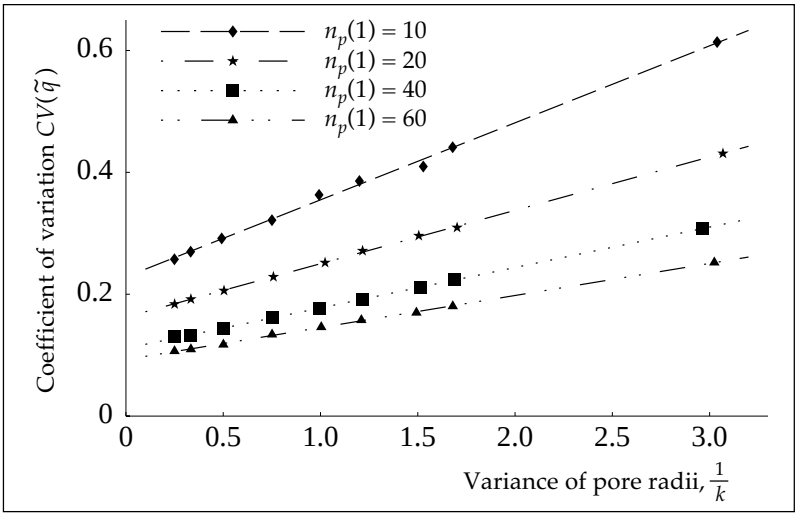

Figure 8. Relationship between coefficient of variation of local flow rate, $CV(\tilde{q})$ and variance of pore radii, $\frac{1}{k}$ for capillary flow. *There is an affine relationship between coefficient of local flow rate and variance of pore radii.*

As for the turbulent flow regime, there is a strong affine relationship between the coefficient of variation of local flow rate and $\frac{1}{k}$, the linear regressions having coefficients of determination greater than 0.997. We note also that the coefficients of variation for capillary flow are around one fifth of those for turbulent flow.

The normalised mean flow rate and coefficient of variation of local flow rate for molecular, or Knudsen, flow are shown in Figures 9 and 10, respectively. Both plots show affine relationships with $\frac{1}{k}$; the coefficients of determination were greater than 0.999 for the mean flow rate, and greater than 0.990 for the coefficient of variation.

3. Conclusions

A simulation has been presented which generates data for the flow of fluids through planar stochastic porous media with gamma distributed pore radii. The simulations allow influence of pore radius distribution on the flow of fluids perpendicular to the plane of the medium to be investigated. The results show that for constant porosity, the mean flow rate is independent of the variance of pore radii for turbulent flow, increases with the second power of variance of pore radii for laminar flow, decreases exponentially for capillary flow and increases linearly for molecular or Knudsen flow. Also, the coefficients of variation of local flow rate exhibit an affine increase with increasing variance of pore radii for each of the above flow modes, though the relationship is weaker for laminar and molecular flow than for turbulent and capillary flow.

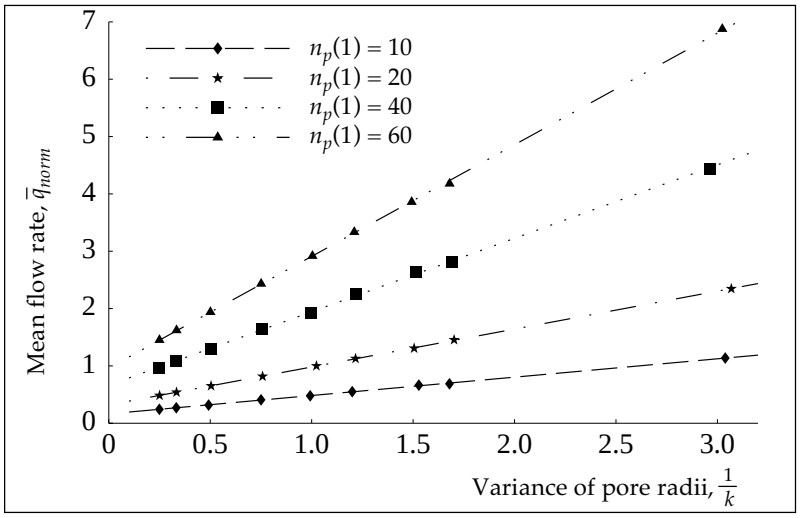

Figure 9. Relationship between normalised mean flow rate, $\overline{q}_{norm}$ and variance of pore radii, $\frac{1}{k}$ for capillary flow. *Mean flow rate decreases exponentially with increasing variance of pore radii.*

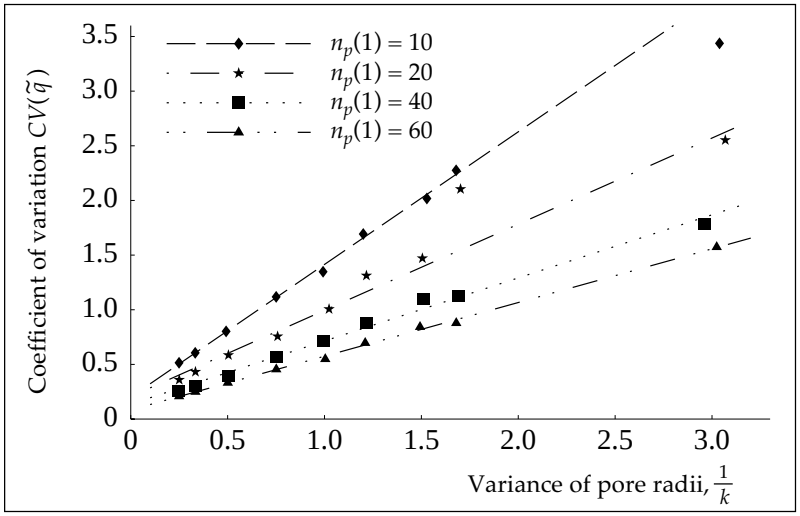

Figure 10. Relationship between coefficient of variation of local flow rate, $CV(\tilde{q})$ and variance of pore radii, $\frac{1}{k}$ for capillary flow. *There is an affine relationship between coefficient of local flow rate and variance of pore radii.*

4. References

[1] Miles, R.E. "Random Polygons Determined by Random Lines in a Plane." *Proceedings of the National Academy of Science*, Vol. 52, pp 901-907, 1157-1160, 1964.

[2] Corte, H. and Lloyd, E.H. "Fluid Flow through Paper and Sheet Structure." In *Consolidation of the Paper Web, Transactions of the Fundamental Research Symposium*, F. Bolam (ed.), Cambridge, 1965. Technical Section of BPBMA, London, 1966, pp 981-1009. See also "Discussion," following, pg 1010.

[3] Deng, M. and Dodson, C.T.J. *Paper: An Engineered Stochastic Structure*. Tappi Press, Atlanta, 1994.

[4] Dodson, C.T.J. and Sampson, W.W. "Spatial Statistics of Stochastic Fibre Networks." *Journal of Statist. Phys.*, Vol. 96, No. 1/2, pp 447-458, 1999.

[5] Dodson, C.T.J. and Sampson, W.W. "Modeling a Class of Stochastic Porous Media." *Applied Math. Lett.*, Vol. 10, No. 2, pp 87-89, 1997.

[6] Dodson, C.T.J. and Sampson, W.W. "The Effect of Paper Formation and Grammage on its Pore Size Distribution." *Journal of Pulp and Paper Science*, Vol. 22, No. 5, pp J165-J169, 1996.

[7] Johnston, P.R. "The Most Probable Pore Size Distribution in Fluid Filter Media." *Journal of Testing and Evaluation*, Vol. 11, No. 2, pp 117-121, 1983.

[8] Johnston, P.R. "Revisiting the Most Probable Pore Size Distribution in Filter Media. The Gamma Distribution." *Filtrn. and Sepn.*, Vol. 35, No. 3, pp 287-292, 1998.

[9] Corte, H. "The Porosity of Paper." Chapter 6 in *Handbook of Paper Science*, H.F. Rance (ed), Elsevier Scientific Publishing, Amsterdam, 1982.

[10] Corte, H. "Bestimmung der Porengrößenverteilung in Papier." *Das Papier*, Vol. 19, No. 7, pp 346-351, 1965.

[11] ASTM Method F316. "Pore Size Characteristics of Membrane Filters by Bubble Point and Mean (Middle) Flow Pore Test."

[12] Foscolo, P.U., Gibilaro, L.G. and Waldram, S.P. "A Unified Model for Particulate Expansion of Fluidised Beds and Flow in Fixed Porous Media." *Chem. Eng. Sci.*, Vol. 38, No. 8, pp 1251-1260, 1983.

[13] Ng, W.K., Sampson, W.W., Dodson, C.T.J. "The Evolution of a Pore Size Distribution in Paper." In *Proceedings of Progress in Paper Physics – A Seminar*, Stockholm, pp 5-7, June 1996.

[14] Sampson, W.W., McAlpin, J., Kropholler, H.W. and Dodson, C.T.J. "Hydrodynamic Smoothing in the Sheet Forming Process." *Journal of Pulp and Paper Science*, Vol. 21, No. 12, pp J422-J426, 1995.

[15] Norman, B., Sjödin, U., Alm, B., Björklund, K., Nilsson, F. and Pfister, J.-L. "The Effect of Localised Dewatering on Paper Formation." In *Proceedings of the TAPPI 1995 International Paper Physics Conference*, Niagara-on-the-Lake, pp 55-59, Tappi Press, Atlanta, 1995.

[16] Dodson, C.T.J. and Scharcanski, J. "Simulating Colloidal Thickening: Virtual Papermaking." *SIMULATION*, Vol. 74, No. 4, pp 200-206, April 2000.

[17] Wolfram, S. *The Mathematica Book*, 3rd edition, Wolfram Media/Cambridge University Press, 1996.

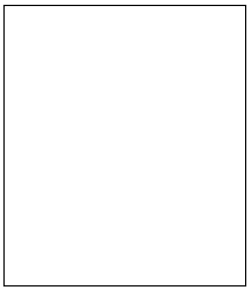

Christopher T.J. Dodson has been a Professor of Mathematics in the Department of Mathematics of the University of Manchester Institute of Science and Technology, United Kingdom, since 1996. From 1989 through 1996, he filled the NSERC Abitibi-Price Senior Research Chair at the University of Toronto in Canada. For 20 years prior to that, he was with the Department of Mathematics of Lancaster University, UK. Dr. Dodson's research interests include differential geometry, stochastic geometry and applications to spacetime structure, stochastic processes and information systems. The books he has published recently include *A User's Guide to Algebraic Topology*, with P.E. Parker; *Tensor Geometry—Graduate Texts in Mathematics 120*, with T. Poston; and *Paper: An Engineered Stochastic Structure*, with M. Deng. His home page is at *www.ma.umist.ac.uk/kd/homepage/dodson.html*.

William W. Sampson received his BSc and PhD degrees in Paper Science from the University of Manchester Institute of Science and Technology, United Kingdom, in 1989 and 1992, respectively. His PhD research focused on the measurement and modelling of the the filtration of fibre suspensions. He has been a Lecturer in the Department of Paper Science at UMIST since 1992. Dr. Sampson's current research interests are in the area of clumping in fibre suspensions, its consequences for the mass and void structure of planar fibre networks formed from suspensions, and flow through networks during and after forming. This work involves the use of statistical geometry and simulation to study the structure of, and structural dependence of flow through, general classes of stochastic fibre networks; the outcomes of these studies are applied to the specific fibre network known as paper. He is a member of the Pulp and Paper Fundamental Research Committee, TAPPI, PITA and APPITA.